Journal of Solid State Chemistry 183 (2010) 1416–1422

Contents lists available at ScienceDirect

Journal of Solid State Chemistry

journal homepage: www.elsevier.com/locate/jssc

MAS-NMR investigations of the crystallization behaviour of lithium aluminum silicate (LAS) glasses containing P_2O_5 and TiO_2 nucleants

A. Ananthanarayanan [a,b], G.P. Kothiyal [a], L. Montagne [b,*], B. Revel [b]

[a] Technical Physics and Prototype Engineering Division, Bhabha Atomic Research Centre, Mumbai 400085, India
[b] Université Lille Nord de France – UMR CNRS 8181, USTL, 59655 Villeneuve d'Ascq, France

ARTICLE INFO

Article history:
Received 25 January 2010
Received in revised form
5 April 2010
Accepted 9 April 2010
Available online 13 April 2010

Keywords:
Glass
Glass ceramics
Lithium alumino-silicate
MAS-NMR
P_2O_5
TiO_2

ABSTRACT

Lithium aluminum silicate (LAS) glass of composition (mol%) $20.4Li_2O–4.0Al_2O_3–68.6SiO_2–3.0K_2O–2.6B_2O_3–0.5P_2O_5–0.9TiO_2$ was prepared by melt quenching. The glass was then nucleated and crystallized based on differential thermal analysis (DTA) data and was characterized by ^{29}Si, ^{31}P, ^{11}B and ^{27}Al MAS-NMR. XRD and ^{29}Si NMR showed that lithium metasilicate (Li_2SiO_3) is the first phase to c form followed by cristobalite (SiO_2) and lithium disilicate ($Li_2Si_2O_5$). ^{29}Si MAS-NMR revealed a change in the network structure already for the glasses nucleated at 550 °C. Since crystalline Li_3PO_4, as observed by ^{31}P MAS-NMR, forms concurrently with the silicate phases, we conclude that crystalline Li_3PO_4 does not act as a nucleating agent for lithium silicate phases. Moreover, ^{31}P NMR indicates the formation of $M–PO_4$ (M=B, Al or Ti) complexes. The presence of BO_3 and BO_4 structural units in all the glass/glass-ceramic samples is revealed through ^{11}B MAS-NMR. B remains in the residual glass and the crystallization of silicate phases causes a reduction in the number of alkali ions available for charge compensation. As a result, the number of trigonally coordinated B (BO_3) increases at the expense of tetrahedrally coordinated B (BO_4). The ^{27}Al MAS-NMR spectra indicate the presence of tetrahedrally coordinated Al species, which are only slightly perturbed by the crystallization.

1. Introduction

Glass-ceramics are polycrystalline materials obtained by controlled crystallization of parent glasses [1]. Depending upon the composition of the parent glass and the heat treatment chosen, various properties of the glass-ceramic such as thermal expansion coefficient (TEC), and micro-hardness (MH) can be precisely controlled [2,3]. One of the most widely studied and commercially utilized glass-ceramic forming systems is the lithium aluminum silicate (LAS) system. LAS glass-ceramics exhibit a wide range of useful properties such as low or even zero thermal expansion coefficient (TEC), good resistance to mechanical and thermal shock and excellent chemical durability [4–7]. As a result these glass-ceramics have found extensive application in heat exchangers, cookware or telescope mirror supports [8,9]. Our aim is to produce glass-ceramics for the sealing applications, especially compressive seals capable of withstanding high pressure.

For all these applications, bulk crystallization is desired. However, LAS glasses have a tendency to surface crystallize if there is no site for heterogeneous nucleation [10]. Therefore, depending upon the composition chosen, LAS glasses have been nucleated by addition of TiO_2, Ta_2O_5, Y_2O_3, CeO_2, F^-, etc. [11–15]. P_2O_5 has been shown to be particularly effective in the low alumina LAS glasses ($Al_2O_3 \leq 12$ wt%) for the bulk crystallization of lithium disilicate [16]. While it is established that P_2O_5 enhances bulk crystallization in LAS glasses, the exact mechanism is still not clear. Headley and Loehman [16] conclusively demonstrated the epitaxial growth of Li_2SiO_3, cristobalite (SiO_2) and $Li_2Si_2O_5$ on Li_3PO_4 crystals using electron microscopy, proving the role of P_2O_5 as a nucleating agent. However, NMR studies carried out on binary lithium silicate compositions with P_2O_5 incorporation also suggest that Li_3PO_4 is not a precursor to $Li_2Si_2O_5$ [17]. The recent MAS-NMR study on multi-component glasses by Goswami et al. [18] also called into question the role of P_2O_5 as a nucleating agent. It was concluded that a silicate phase separation occurs prior to crystallization, which may be induced by P_2O_5. We have previously carried out detailed NMR studies on phase emergence in LAS glasses of composition (wt%) $xLi_2O–71.7SiO_2–(17.7-x)Al_2O_3–4.9K_2O–3.2B_2O_3–2.5P_2O_5$ ($5.1 \leq x \leq 12.6$) and have observed the emergence of $(Li/K)BSi_2O_6$ phase similar to virgilite ($Li_xAl_xSi_{3-x}O_6$) in the high alumina content ($x \leq 8.8$) glass-ceramics [19]. This boro-silicate phase could not be identified with XRD, thus again validating the complementary utility of NMR to XRD in characterization of glass-ceramics. The effect of TiO_2 addition on LAS glasses nucleated by

* Corresponding author.
E-mail address: lionel.montagne@univ-lille1.fr (L. Montagne).

0022-4596/$ - see front matter © 2010 Elsevier Inc. All rights reserved.
doi:10.1016/j.jssc.2010.04.011

P_2O_5 investigated by Arvind et al. [20], report that P_2O_5 incorporation helps in the crystallization of lithium silicate phases while TiO_2 mitigates the formation of quartz, leading to the formation of single phase glass-ceramics. However, Li_3PO_4 crystals were not detected by XRD in this study [20]. In the present paper, we have studied the effect of different heat treatment schedules on LAS glasses containing both P_2O_5 and TiO_2 of composition (mol%) $20.4Li_2O–4.0Al_2O_3–68.6SiO_2–3.0K_2O–2.6B_2O_3–0.5P_2O_5–0.9TiO_2$ using X-ray diffraction (XRD), ^{29}Si, ^{31}P, ^{11}B and ^{27}Al MAS-NMR for structural characterization. This particular composition was chosen owing to its propensity to yield single phase lithium disilicate glass-ceramics. Our aim is to investigate the conjugated effect of P_2O_5 and TiO_2 on the crystallization behaviour of this multi-component glass.

2. Experimental procedure

LAS glass of composition (mol%) $20.4Li_2O–4.0Al_2O_3–68.6SiO_2–3.0K_2O–2.6B_2O_3–0.5P_2O_5–0.9TiO_2$ was prepared by the melt quench technique. Analytical grade precursors (Li_2CO_3, Al_2O_3, SiO_2, B_2O_3, $NH_4H_2PO_4$ and KNO_3 and TiO_2) were mixed thoroughly and calcined in recrystallized alumina crucibles according to a schedule determined by the decomposition temperatures of the precursors. To ensure complete decomposition of the precursors, the batch was weighed before and after calcination to ascertain weight loss. The calcined batch was melted under air ambient at 1500–1550 °C in a covered Pt–Rh crucible in a raising lowering hearth electric furnace (Model OKAY, M/s Bysakh and Co., Kolkata) and held for 1–2 h to ensure melt homogenization. After homogenization, the melt was poured onto pre-heated graphite moulds and annealed at 500 °C for 3–4 h to relieve thermal stresses. The vitreous nature of the annealed glass was verified using powder XRD (Philips PW1710 X-ray Diffractometer with collimated Cu$K\alpha$ radiation).

Based on previous DTA studies [21], samples were nucleated at 550 °C and subsequently heated at 60 °C/h to 650–800 °C, and held there for 2 h, followed by furnace cooling to room temperature. The crystallization heat treatments are summarized in Table 1. Powder XRD in the $20^\circ \le 2\theta \le 70^\circ$ range in steps of 0.5° was used to identify the crystalline phases formed. Phase identification was carried out using MATCH® software.

^{29}Si, ^{31}P, ^{27}Al and ^{11}B MAS-NMR spectra were recorded at 2.34, 9.4, 18.8 and 18.8 T, respectively, on Bruker AVANCE spectrometers, with 4 mm probes at 12.5 kHz spinning speed, except for ^{29}Si for which a 7 mm probe at 8 kHz was used. The Larmor frequencies were 19.8, 161.9, 208.5 and 256.8 MHz for ^{29}Si, ^{31}P, ^{27}Al and ^{11}B, respectively. For ^{31}P, the pulse duration was 1.6 μs ($\pi/6$), and the recycle delay was 120 s. For ^{11}B, the pulse duration was 2 μs ($\pi/6$), and the recycle delay was 10 s. For ^{27}Al, the pulse duration was 1.5 μs ($\pi/8$), and the recycle delay was 2 s. For ^{29}Si, the pulse duration was 1.6 μs ($\pi/5$), and the recycle delay was 180 s. This delay is sufficient to allow detection of Si containing phases, although it might be insufficient for reliable phase quantification, which is not the aim of this study. All relaxation delays were chosen long enough to enable relaxation at the field strength that was used. The ^{29}Si chemical shifts are relative to tetramethyl silane (TMS) at 0 ppm, those of ^{27}Al are relative to $Al(H_2O)_6^{3+}$ species at 0 ppm in 1 M $Al(NO_3)_3$ solution , those of ^{11}B nuclei are given relative to BPO_4 at 3.6 ppm and those of ^{31}P are relative to 85% H_3PO_4 at 0 ppm. The decomposition of NMR spectra was carried out using DM-FIT software [22]. We fitted ^{29}Si and ^{31}P NMR glass spectra using a Gaussian lineshape that reflects the distribution of chemical shifts due to disorder, while a predominantly Lorentzian lineshape was found more suitable for the crystalline phases observed in the glass-ceramic samples.

3. Results

3.1. XRD

The X-ray diffractograms of the LAS glass heat treated at various temperatures are given in Fig. 1. In the as prepared sample and that nucleated at 550 °C, XRD patterns show the broad peak characteristic of amorphous materials. The diffractogram of the sample heat-treated at 650 °C shows characteristic peaks of lithium metasilicate (PDF 29-0829) superimposed on an amorphous background. The sample heat treated at 740 °C, shows in addition to lithium metasilicate, peaks corresponding to cristobalite (SiO_2) (PDF 76-0941). When the sample was heat treated at 820 °C, only peaks corresponding to lithium disilicate (PDF 40-0376) were observed. The phase emergence at different temperatures is collated in Table 2 and some thermo-physical properties are presented in Table 3.

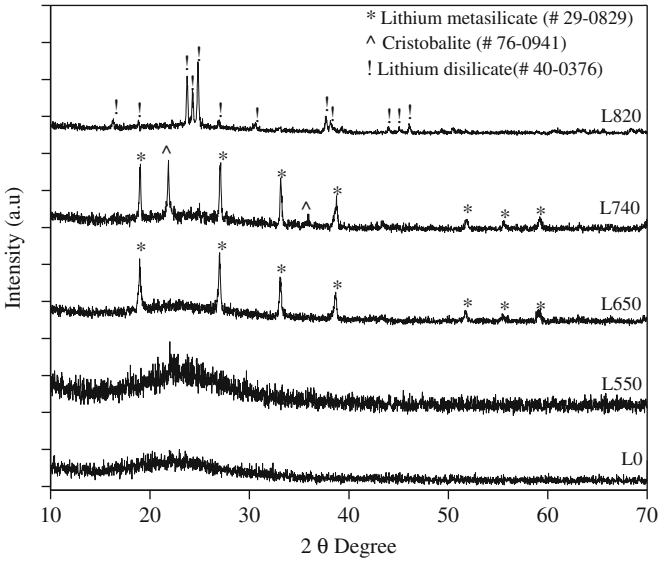

Fig. 1. XRD patterns of lithium aluminum silicate (LAS) glass sample heat treated according to Table 1.

Table 1
Heat treatments applied to LAS glass samples and their nomenclatures.

Sample name	Nucleation temperature (°C)	Dwell time (h)	Crystallization temperature (°C)	Dwell time (h)
L0	As prepared sample			
L550	550	1	Nucleated sample	
L650	550	1	650	2
L740	550	1	740	2
L820	550	1	820	2

Table 2
Chronology of phase emergence in the LAS glasses.

Temperature (°C)	Phases in LAS glass-ceramics
650	LS
710	LS
740	LS, CR
770	LS, CR
800	LS, CR, LS2
820	LS2

LS=lithium metasilicate, Q=quartz, CR=cristobalite, and LS2=lithium disilicate.

Table 3
TEC, T_g, T_{ds} and microhardness (MH) a function of heat-treatment temperature.

Crystallization temperature (°C)	TEC/ $\times 10^{-6}$ °C^{-1} ± 5%	MH (GPa)	$T_g \pm 2$ (°C)	$T_{ds} \pm 2$ (°C)
650	9.3	6.02 ± 0.04	563	647
740	15.3	7.32 ± 0.03	502	626
820	8.6	8.87 ± 0.03	500	818

The error in MH are standard deviation from mean calculated from at least 10 measurements.

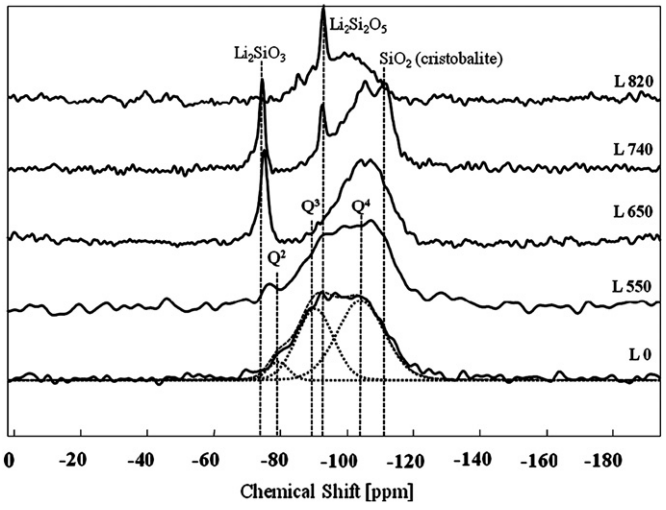

Fig. 2. ^{29}Si MAS-NMR spectra of LAS glass heat treated at various temperatures according to Table 1. Typical spectrum decomposition is shown for L0 glass. The estimated positions of Q^2, Q^3 and Q^4 resonances are indicated.

3.2. ^{29}Si MAS-NMR

The ^{29}Si spectra of the LAS glass heat treated at different temperatures are presented in Fig. 2. The spectra of the as prepared glass (L0) and that nucleated at 550 °C (L550) both show a broad feature in the −70 to −120 ppm range, indicating the amorphous nature of these samples. The spectrum of L0 sample can be decomposed into three resonances at −79, −91 and −104 ppm attributed to Q^2, Q^3 and Q^4 structural units, respectively, as found in other aluminosilicate glasses [23–26]. While the spectra of L550 and L0 are amorphous in character, the shape of the broad feature is changed, indicating that the glass network is already modified by the heat treatment at 550 °C. Further, Fig. 2 clearly shows an increase of the Q^4 resonance and a decrease of the Q^3 resonance. Moreover, the Q^2 resonance shifts to a value of ∼−77 ppm, which is close to the chemical shift of lithium metasilicate [27].

In the sample heat treated at 650 °C (L650), a sharp resonance is clearly observed at −75 ppm, corresponding to lithium metasilicate crystals [27], in agreement with XRD. The crystallization of lithium metasilicate containing silicon in Q^2 configuration enhances polymerization of the residual glass, thus leading to the shift of the ^{29}Si resonance of the residual glass to more negative values.

At 740 °C (L740), in addition to the peak at −75 ppm, two new resonances are evident at ∼−92 and −110 ppm that can be assigned to lithium disilicate and cristobalite, respectively [28,29]. Interestingly, the lithium disilicate is not discernible in the XRD pattern of L740 glass-ceramics (Fig. 1). The broad amorphous background due to the residual glass does not change significantly compared to the spectrum of the L650 sample.

Upon heat treating at 820 °C (L820), only the resonance corresponding to lithium disilicate at −92 ppm [28] is evident. This proves conclusively that the L820 glass-ceramic is composed of single phase lithium disilicate, confirming the XRD analysis (Fig. 1). Further, a change in the shape of the amorphous background is observed along with a shift to less negative chemical shifts as compared to L740 samples.

3.3. ^{31}P MAS-NMR

The ^{31}P MAS-NMR spectra of the LAS glass heat treated at different temperatures are displayed in Fig. 3. To observe changes in the crystallinity of the phosphate phase closely, we have recorded ^{31}P NMR spectra for LAS glasses heat treated at 610 °C (L610) and 630 °C (L630). The spectra of the as prepared glass (L0), those heat treated at 550 °C (L550) and heat treated at 610 °C (L610) are nearly identical. The broad resonances centered on 9 and 2 ppm are indicative of the amorphous environment around the P atoms. The resonance at 9 ppm can be assigned to orthophosphate (Q^0) groups [30], in accordance with the chemical shift of Li_3PO_4 and K_3PO_4 at 10.4 and 11.7 ppm [31,32], respectively. Since the ^{31}P chemical shift is very sensitive to the field strength of charge compensating cation of the PO_4^{3-} structural units, the chemical shift at 9 ppm indicates that cations other than K^+ and Li^+ assume the role of charge compensation. These may be Ti^{4+}, Al^{3+} or B^{3+}. In addition, the ^{31}P spectra contain a broad resonance centered on 0 ppm. This could arise from the presence of Q^1 groups, as observed in other silicate glasses containing P_2O_5 [30]. In silicate glasses containing P_2O_5, B_2O_3, Al_2O_3 and TiO_2, connections between phosphate groups and the glass network were revealed through ^{31}P resonances in the −4 to −8 ppm region that indicated the

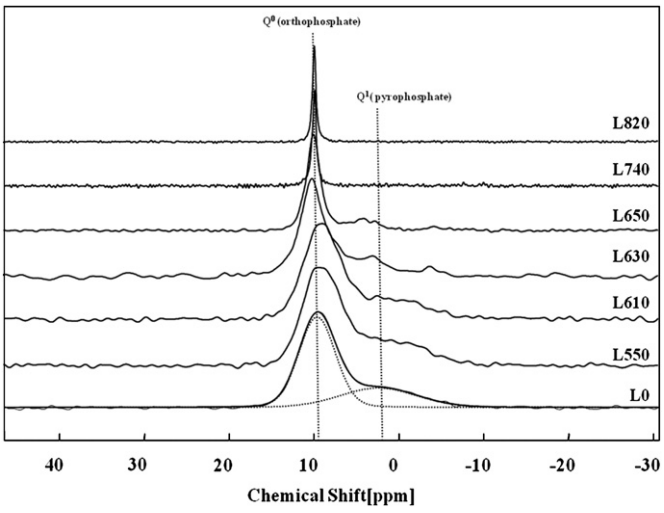

Fig. 3. ^{31}P MAS-NMR spectra of LAS glass heat treated at various temperatures according to Table 1.

presence of P–O–Al [33], P–O–B [34,35] or P–O–Ti [36] bonds that can be considered as Q^1 sites. In the sample heat treated at 630 °C (L630), the Q^0 resonance shifts from 9 to 10 ppm and becomes sharper, indicating the onset of orthophosphate crystallization. As the crystallization temperature increases to 650, 740 and 820 °C for L650, L740 and L820 samples, respectively, the resonance at ~10 ppm becomes even sharper indicating the increasing crystallinity of the orthophosphate phase. The chemical shift of the resonance is very close to that of pure Li_3PO_4 [31], implying that the large quantity of Li_2O in the glass composition precludes the crystallization of a mixed $(Li,K)_3PO_4$ phase that we had observed in similar glasses containing a lesser quantity of Li_2O [19]. We notice that the Li_3PO_4 crystals observed in NMR spectra are not detected by XRD (Fig. 1), thus validating the interest of complimentary NMR analysis. This is discussed later in conjunction with the XRD results.

3.4. ^{27}Al MAS-NMR

The ^{27}Al MAS-NMR spectra of the LAS glass heat treated at different temperatures are shown in Fig. 4. When ^{27}Al MAS-NMR spectra are collected at 18.8 T, the effects of quadrupolar broadening are significantly reduced leading to nearly Gaussian lineshapes (Fig. 4). The spectra show a single peak in the 55–60 ppm region, attributed to Al(4) [37,38]. The ^{27}Al resonances remain unaffected by the thermal treatment and no sharp resonances are evident, precluding the crystallization of an Al containing phase. However, a closer inspection reveals a small shift in the resonance to less positive values for samples heated at 650 and 740 °C and a narrowing of the resonance in the latter case.

3.5. ^{11}B MAS-NMR

The ^{11}B NMR spectra of the LAS glass heat treated at different temperatures, collected at 18.8 T, are shown in Fig. 5. At this static magnetic field the effect of second order quadrupolar broadening is considerably mitigated and the BO_3 and BO_4 peaks are clearly resolved. The spectra consist of two groups of resonances centered at ~10 to 15 ppm and ~−5 to 0 ppm, which can be assigned to BO_3 and BO_4 units, respectively [39]. In addition, in Fig. 5 it is observed that two different types of BO_3 and BO_4 sites contribute to the overall BO_3 and BO_4 resonances. The BO_3 resonance includes contributions from peaks at ~15 and 10 ppm. The former are due to BO_3 symmetric sites containing three bridging or non-bridging oxygen atoms (referred to as BO_3sym), while the later result from BO_3 asymmetric sites, each containing one or two bridged oxygen atoms (referred to as BO_3asym) [39], which are unlikely in the glass reported here. Further, the resonances are broad precluding the presence of any crystalline boron containing phase that would be revealed by the presence of sharp resonance [19]. In Fig. 5 it is evident that the spectra of L0 and L550 samples are almost identical while for the sample heat treated at 650 °C (L650), the ^{11}B NMR spectrum shows considerable change. The BO_3 fraction indeed increases at the expense of BO_4 and the fraction of BO_3asym increases and becomes more abundant than BO_3sym. Interestingly, in the sample heat treated at 740 °C (L740), the BO_4 resonance shows a contribution at ~0 ppm (marked as BO_4^* in Fig. 5). This is attributed to B coordinated to 1 B and 3 Si as will be discussed in detail subsequently. The intensity of the BO_4 resonance at 0 ppm increases upon heat treatment at 820 °C.

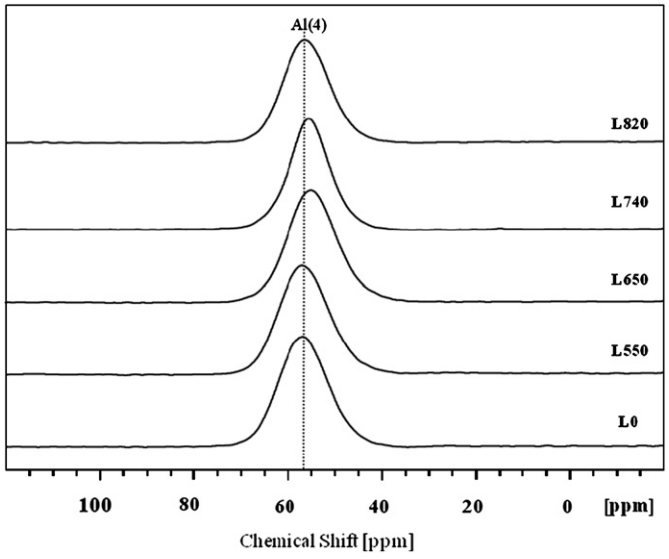

Fig. 4. ^{27}Al MAS-NMR of LAS glass heat treated at various temperatures according to Table 1, recorded at 18.8 T.

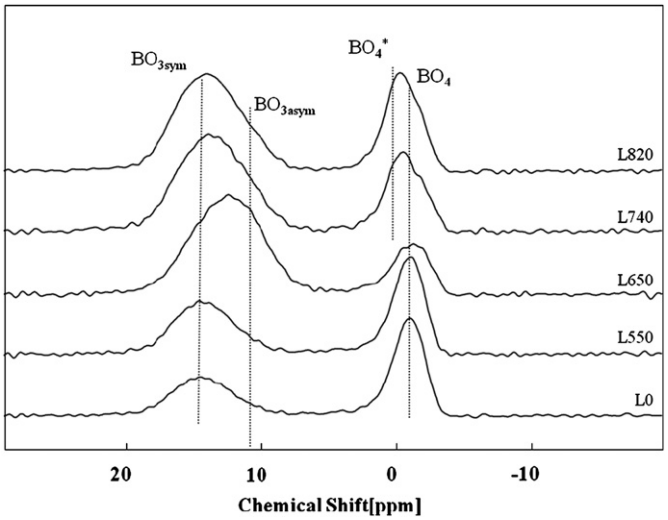

Fig. 5. ^{11}B NMR spectra of LAS glass heat treated at various temperatures according to Table 1, recorded at 18.8 T.

4. Discussion

In glass-ceramics, the nature and relative fractions of phases strongly affect the thermo-physical properties. Thus, a complete understanding of the glass-ceramics' behaviour necessitates the characterization not only of crystalline phases but also of the residual glass. Complementary to XRD, which is the most common method for crystalline phase identification, NMR is a powerful tool for such study because it enables the characterization of both amorphous and crystalline phases, the observation of each nucleus separately (particularly light elements like boron, which are difficult to observe in crystals with XRD), the detection of phases present in very low amount, and the quantification of the proportion of crystals and amorphous phases. Moreover, the use of a high-field (18.8 T) NMR spectrometer enables us to obtain an improved sensitivity and resolution especially for quadrupolar nuclei like ^{27}Al and ^{11}B.

In the following discussion, we use the NMR results to describe the crystallization process of an LAS glass containing both P_2O_5 and TiO_2. We focus our attention on the evolution of the residual glass, where valuable information can be gleaned through NMR. In our previous study [20] on LAS glasses nucleated by P_2O_5 and TiO_2, it was observed using XRD that lithium metasilicate is the

first phase to form at ~650 °C followed by cristobalite at ~740 °C, and finally lithium dislicate forms at ~800 °C. The samples crystallized at 820 °C were composed entirely of lithium disilicate. We had concluded that P_2O_5 incorporation helps in the crystallization of lithium silicate phases while TiO_2 mitigates the formation of quartz, leading to the formation of single phase glass-ceramics. In the present report, we focus on a single composition in order to get deeper insights into the phase evolution during the thermal treatment. The ^{29}Si MAS-NMR spectra (Fig. 2) corroborate the X-ray diffractograms and it also brings further information. Indeed, after the nucleation heat treatment, NMR reveals that the Q^4 contribution in L550 increases compared to L0 sample. In addition, the Q^2 resonance of the L550 sample is shifted to less negative values compared to L0 sample (~ −77 ppm) which is close to that of crystalline lithium metasilicate (−75 ppm) [27]. Similar increase in the network polymerization and a shift of Q^2 resonance to a value near that of crystalline lithium metasilicate was observed by Clayden et al. [40] in binary lithium silicate glasses heat treated at 500 °C. Since there is no evidence for crystallization, the change in network polymerization can be attributed to formation of atomic scale inhomogenities. These are regions that are enriched in alkali species compared to the surrounding glass and are consequently less polymerized. Crystallization can occur more easily in the regions of lower polymerization and it is likely that Li_2SiO_3 first crystallizes in such regions [40]. Concurrently, it must be emphasized that crystalline nuclei are not observed at this stage of the process. It is also possible that this could be the beginning of crystal growth and that the crystalline fraction is below the detection threshold of XRD and NMR. The heat treatment at 650 °C results in the crystallization of lithium metasilicate, from which we can deduce that the fraction of Li_2O in the residual glass decreases. From the continuous random network theory [41], it is known that Li_2O is a network modifying oxide, the reduction of which increases the polymerization of the glass network. This is evident in the ^{29}Si NMR spectrum of the residual glass of L650 sample that shows an increase of polymerization since the residual glass resonance is now centered on −110 ppm. In L740 samples, crystallization of lithium disilicate and cristobalite is evidenced by the sharp resonances at −92 and −110 ppm [28,29].

In the L820 sample, lithium disilicate is the only phase evident. No more lithium metasilicate is observed probably because at this temperature, lithium disilicate forms by the reaction of SiO_2 (from cristobalite or the residual glass) with lithium metasilicate as given below:

$$Li_2SiO_3 + SiO_2 \rightarrow Li_2Si_2O_5$$

Headley and Loehman [16] showed using electron microscopy that the Li_2SiO_3 and cristobalite (SiO_2) in the above reaction grow epitaxially on crystals of Li_3PO_4. We may then expect that crystalline Li_3PO_4 would be observed before the crystallization of the major silicate phases. However, when the ^{31}P MAS-NMR spectra are considered, it is observed that the orthophosphate peak (at ~10 ppm) develops in conjunction with the major silicate phases observed in XRD and ^{29}Si NMR (Figs. 1 and 2, respectively). The ^{31}P spectra of both the parent glass and the glasses nucleated at 550 °C and the glass heat treated at 610 °C are similar, indicating the similarity in the environment about the P atoms in these samples. By 630 °C, the orthophosphate resonance narrows compared to the sample heat treated at 610 °C. This indicates the increasing crystallinity of Li_3PO_4 present in the glass. It is interesting to compare the ^{31}P NMR spectrum of the as prepared glass with that of another LAS glass of composition (mol%) $20.5Li_2O$–$4.0Al_2O_3$–$68.9SiO_2$–$3.0K_2O$–$2.7B_2O_3$–$1.0P_2O_5$ as shown in Fig. 6. This glass was referred to as LAS-P in our previous investigation [20]. Since the glass reported here (LAS-PT) contains a lower concentration of P_2O_5, it is expected to contain a lower fraction of Q^1 pyrophosphate structural units as compared to LAS-P, since it was reported that the lower fraction of P_2O_5 would result in lower fraction of pyrophosphate (Q^1) units [42]. However, in Fig. 6 the large fraction of Q^1 units in the present (LAS-PT) glass is readily evident. As mentioned in the Results section, the resonance centered at 0 ppm indicates the presence of P–O–Al [33] P–O–B [34,35] or P–O–Ti [36] bonds. Since the glass investigated here differs from LAS-P only with regards to the incorporation of TiO_2, it is most likely that the formation of P–O–Ti complexes is responsible for the enhanced intensity of the 0 ppm resonance as compared to LAS-P [36].

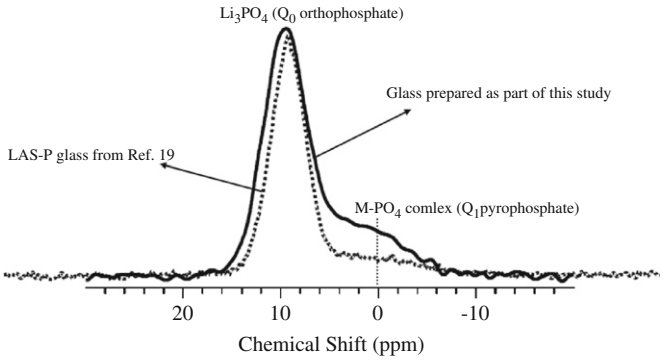

Fig. 6. ^{31}P MAS-NMR spectra of LAS glass prepared in this study as compared to a similar LAS glass from Ref. [19]. The glass reported in Ref. [19] contains 1.0 mol% P_2O_5 as compared to the glass of this study that contains 0.5 mol%.

As temperature at which the glass is heat treated increases from 650 to 800 °C, the crystallinity of the Li_3PO_4 phase increases. The emergence of crystalline Li_3PO_4 concurrently with the Li_2SiO_3 and SiO_2 phases indicates that it is not a precursor for Li_2SiO_3 and SiO_2 (cristobalite) as previously expected. This agrees well with the results of Holland et al. [17] whose NMR investigations have concluded that Li_3PO_4 is not the predecessor phase to lithium silicate. Our observations are also in agreement with the results of Goswami et al. [18] whose observations indicate that crystalline Li_3PO_4 is not a nucleating agent for complex lithium–zinc–silicate glasses.

The ^{27}Al MAS-NMR spectra (Fig. 4) show very little variation in glasses and glass-ceramics. The dominant contribution to the spectrum in all cases is from the peak at ~55 ppm that is assigned to tetrahedrally coordinated Al (Al(4)) as mentioned in the Results section. The presently chosen composition is highly peralkaline ($Al_2O_3/Li_2O = 0.19 < 1$). The large fraction of alkali ions means that Al(4) is energetically stable. In such coordination, the Al^{3+} ions strengthen the glass network and mitigate crystallization during melt quenching. The presence of any other Al coordination, Al(5) and Al(6), is ruled out by means of ^{27}Al MAS-NMR spectra recorded at 18.8 T. The NMR spectra in conjunction with XRD indicate that Al does not participate in the formation of crystalline phases. Although all the spectra seem featureless, a closer inspection reveals that ^{27}Al resonance shifts to less positive values in samples L650 and L740 and a narrowing of the resonance in the latter case. This is an indirect effect of the crystallization of the lithium silicate phases, especially since crystallization of Al containing phase is not observed. We have already observed in Fig. 2 that the crystallization induces an increase in the polymerization of the residual glass and thereby modifies the ^{27}Al chemical shift [37,38].

The ^{11}B MAS-NMR spectra however, show a considerable variation with heat treatment. The ^{11}B MAS-NMR spectra show a change at 650 °C (L650). At this temperature, lithium metasilicate

phase is crystallized as seen in the XRD and ^{29}Si MAS-NMR spectra (Figs. 1 and 2). The formation of this phase reduces the alkali oxide content of the residual glass. Since the ^{11}B NMR spectra do not show any sharp peaks, it is certain that B remains in the residual glass. The reduction in the number of charge compensating cations leads to the following change in the coordination of B atoms [43]. Since the BO_4^- requires the presence of alkali oxides for charge compensation.

$$BO_4 \leftrightarrow BO_3\text{sym} + \text{NBO}$$

The conversion of BO_4 to BO_3 causes the observed reduction in the BO_4 fraction. The non-bridging oxygen (NBO) atom created in (2) may then convert the symmetric BO_3 structural units into an asymmetric BO_3 structural unit as evident in the ^{11}B spectra of the L650 sample. This is given below:

$$BO_3\text{sym} + \text{NBO} \leftrightarrow BO_3\text{asym}$$

Interestingly, by 740 °C, two different BO_4 sites are also evident (a new one evident at $\sim$0 ppm in addition to the resonance at -5 ppm). This is probably a BO_4 structural unit coordinated with 1B and 3Si atoms, while the original BO_4 sites at ~ -5 ppm corresponds to a BO_4 structural unit coordinated with 4Si atoms [39]. As the alkali silicate phases form, the fraction of Si relative to B in the residual glass also decreases. As a result of this, the probability of having a B–O–B linkage increases. The emergence of the peak at $\sim$0 ppm is an indication of the changing structure of the residual glass. This is further corroborated by the reduction in glass transition temperature (T_g) of the L740 glass-ceramic sample (Table 3) indicating the reduction of Si in the residual glass. ^{31}P NMR shows that phosphates are participating in the crystallization process. There is indeed no more evidence for the presence of amorphous phosphate phase at 740 and 820 °C. The observed chemical shift indicates the presence of only Li_3PO_4 crystals, whereas mixed (Li, K) orthophosphate are present before crystallization, together with a significant quantity of Q^1 sites connected through P–O–Al, P–O–B or P–O–Ti bonds. It is however not clear if the disappearance of the Q^1 sites upon crystallization is a consequence of glass network reorganization (like the observed boron evolution), or if it may be at the origin of the network evolution prior to crystallization. However, the observed evolution of the network structure on the ^{29}Si spectrum of L550 prior to the Q^1 dissipation seems to indicate that the phosphates do not participate in the nucleation process.

5. Conclusions

The use of MAS-NMR allowed us to characterize amorphous and crystalline phases that are formed during the entire crystallization process of a complex multi-component glass. ^{29}Si MAS-NMR confirms that heat treatment at 820 °C results in a single phase glass-ceramic composed entirely of lithium disilicate. In addition, the use of NMR allowed us to observe already a change in the network structure of glasses nucleated at 550 °C, thus possibly indicating the formation of inhomogenities or nuclei in the glass. The ^{31}P MAS-NMR spectra indicated that the crystalline phosphate (Li_3PO_4) phase develops in conjunction with the primary crystalline silicate phases, which indicates that crystalline Li_3PO_4 does not act as nucleation sites in the LAS glasses studied. The unchanging nature of the ^{27}Al spectra indicate that Al is tetrahedrally coordinated in all cases and a small shift in the position of the resonance occurs with crystallization of the major silicate phases. The ^{11}B MAS-NMR spectra show significant changes with the crystallization of silicate phases. Although the boron atoms do not participate in the crystallization process, their coordination evolves as a consequence of the modification of the polymerization of the residual glass matrix.

Acknowledgments

The authors thank Dr. J.V. Yakhmi for encouragement and support. They would like to thank Mr. V.K. Shrikhande and Dr. Madhumita Goswami for technical discussion and Mr. Arjun Sarkar for help in preparation of samples. The FEDER, Region Nord Pas-de-Calais, Ministère de l'Education Nationale de l'Enseignement Superieur et de la Recherche, CNRS, and USTL are acknowledged for funding of NMR spectrometers. One of the authors (AA) thanks the DAE for awarding him a fellowship. The authors also thank the IFCPAR for funding the research vide project no. 4008-1.

References

[1] P.W. McMillan, Glass-Ceramics, Academic Press, 1977 p. 1.
[2] P. Riello, P. Canton, N. Comelato, S. Polizi, M. Verità, G. Fagherazzi, H. Hofmeister, S. Hopfe, Nucleation and crystallization behaviour of glass-ceramic material in the Li_2O–Al_2O_3–SiO_2 system of interest for their transparency properties, J. Non-Cryst. Solids 288 (2001) 127–139.
[3] G.A. Khater, M.H. Idris, Role of TiO_2 and ZrO_2 on the crystallizing phases and microstructure in Li, Ba aluminosilicate glass, Ceram. Int. 33 (2007) 233–238.
[4] P.F. James, Glass-ceramic: new compositions and uses, J. Non-Cryst. Solids 181 (1995) 1–15.
[5] M. Chatterjee, M.K. Naskar, Sol–gel synthesis of lithium aluminum silicate powders: the effect of silica source, Ceram. Int. 32 (2006) 623–632.
[6] K. Cheng, Determining crystallization kinetic parameters of Li_2O–Al_2O_3–SiO_2 glass from derivative differential thermal analysis curves, Mater. Sci. Eng. B 60 (1999) 194–199.
[7] P.A. Tick, N.F. Borrelli, I.M. Reaney, Relationship between structure and transparency in glass-ceramic materials, Opt. Mater. 15 (1) (2000) 81–91.
[8] Y.M. Sung, S.A. Dunn, J.A. Koutsky, The effect of boria and titania addition on the crystallization and sintering behaviour of Li_2O–Al_2O_3–$4SiO_2$ glass, J. Eur. Ceram. Soc. 14 (1994) 455–462.
[9] H. Scheidler, J. Thürk, The ceran-top-system®: high tech appliance for the kitchen, in: H. Bach (Ed.), Low Thermal Expansion Glass-Ceramics, Springer Verlag, Berlin, 1995, pp. 51–60.
[10] X. Guo, H. Yang, M. Cao, Nucleation and crystallization behavior of Li_2O–Al_2O_3–SiO_2 system glass-ceramic containing little fluorine and no-fluorine, J. Non-Cryst. Solids 351 (2005) 2133–2137.
[11] J.Y. Hsu, R.F. Speyer, Comparison of the effects of titania and tantalum oxide nucleating agents on the crystallization of Li_2O–Al_2O_3–$6SiO_2$ glasses, J. Am. Ceram. Soc. 72 (12) (1989) 2334–2341.
[12] K. Cheng, Carbon effects on the crystallization of Li_2O–Al_2O_3–SiO_2 glasses, J. Non-Cryst. Solids 238 (1–2) (1998) 152–157.
[13] Y.M. Sung, S.A. Dunn, J.A. Koutsky, The effect of boria and titania addition on the crystallization and sintering behaviour of Li_2O–Al_2O_3–$4SiO_2$ glass, J. Eur. Ceram. Soc. 14 (1994) 455–462.
[14] A.M. Hu, K.M. Liang, F. Zhou, G.L. Wang, P. Weng, Phase transformation of Li_2O–Al_2O_3–SiO_2 glasses with CeO_2 addition, Ceram. Int. 31 (2005) 11–14.
[15] X. Guo, H. Yang, C. Han, F. Song, Crystallization and microstructure of Li_2O–Al_2O_3–SiO_2 glass containing complex nucleating agent, Thermochim. Acta 444 (2006) 201–205.
[16] T.J. Headley, R.J. Loehman, Crystallization of a glass-ceramics by epitaxial growth, J. Am. Ceram. Soc. 67 (9) (1984) 354–361.
[17] D. Holland, Y. Iqbal, P. James, B. Lee, Early stages of crystallisation of lithium disilicate glasses containing P_2O_5—an NMR study, J. Non-Cryst. Solids 232–234 (1998) 140–146.
[18] M. Goswami, G.P. Kothiyal, L. Montagne, L. Delevoye, MAS-NMR study of lithium zinc silicate glasses and glass-ceramics with various ZnO content, J. Solid State Chem. 181 (2008) 269–275.
[19] A. Ananthanarayanan, G.P. Kothiyal, L. Montagne, B. Revel, MAS-NMR studies of lithium aluminum silicate (LAS) glasses and glass-ceramics having different Li_2O/Al_2O_3 ratio, J. Solid State Chem. 183 (2010) 120–127.
[20] A. Arvind, A. Sarkar, V.K. Shrikhande, A.K. Tyagi, G.P. Kothiyal, The effect of TiO_2 addition on the crystallization and phase formation in lithium aluminum silicate (LAS) glasses nucleated by P_2O_5, J. Phys. Chem. Solids 69 (11) (2008) 2622–2627.
[21] A. Arvind, A. Dixit, R.K. Lenka, R.D. Purohit, V.K. Shrikhande, G.P. Kothiyal, Some studies on the phase formation and kinetics in TiO_2 containing lithium aluminum silicate (LAS) glasses nucleated by P_2O_5, J. Therm. Anal. Cal., in press.
[22] D. Massiot, F. Fayon, M. Capron, I. King, S. Le Calve, B. Alonso, J.O. Durand, B. Bujoli, Z. Gan, G. Hoatson, Modelling one- and two-dimensional solid-state NMR spectra, Magn. Reson. Chem. 40 (2002) 70–76.

[23] B.G. Parkinson, D. Holland, M.E. Smith, A.P. Howes, C.R. Scales, The effect of Cs_2O additions on HLW wasteform glasses, J. Non-Cryst. Solids 351 (2005) 2425–2432.
[24] J. Ramkumar, V. Sudarsan, S. Chandramouleeswaran, V.K. Shrikhande, G.P. Kothiyal, P.V. Ravindran, S.K. Kulsreshta, T. Mukherjee, Structural studies on boroaluminosilicate glasses, J. Non-Cryst. Solids 354 (2008) 1591–1597.
[25] A. Hamoudi, L. Kouchaf, C. Depecker, B. Revel, L. Montagne, P. Cordier, Microstructural evolution of amorphous silica following alkali–silica reaction, J. Non-Cryst. Solids 354 (2008) 5074–5078.
[26] H. Maekawa, T. Maekawa, K. Kawamura, T. Yokokawa, The structural groups of alkali silicate glasses determined from ^{29}Si MAS-NMR, J. Non-Cryst. Solids 127 (1991) 53–64.
[27] K.J.D. MacKenzie, M.E. Smith, Multinuclear Solid State NMR of Inorganic Materials, Pergamon, 2002 p. 212.
[28] Y. Iqbal, W.E. Lee, D. Holland, P. James, Metastable phase formation in the early stages of crystallization of lithium disilicate glass, J. Non-Cryst. Solids 224 (1998) 1–16.
[29] G. Engelhardt, R. Radeglia, A semi-empirical quantum-chemical rationalization of the correlation between Si–O–Si angles and ^{29}Si NMR chemical shifts of silica frameworks and framework aluminosilicates (Zeolites), J. Chem. Phys. Lett. 108 (3) (1984) 271–274.
[30] G.D. Cody, B. Mysen, G. Sághi-Szabó, J.A. Tossell, Silicate-phosphate interactions in silicate glasses and melts: I. A multinuclear (^{27}Al, ^{29}Si, ^{31}P) MAS NMR and ab initio chemical shielding (^{31}P) study of phosphorous speciation in silicate glasses, Geochim. Cosmochim. Acta 65 (14) (2001) 2395–2411.
[31] R. Dupree, D. Holland, M.G. Mortuza, A MAS-NMR investigation of lithium silicate glasses and glass ceramics, J. Non-Cryst. Solids 116 (1990) 148–160.
[32] A.R. Grimer, U. Haubenreisser, High field static and MAS ^{31}P NMR: chemical shift tensors of polycrystalline potassium phosphates $P_2O_5 \cdot xK_2O$ ($0 \le x \le 3$), Chem. Phys. Lett. 99 (1983) 487–490.
[33] R.G. Hill, A. Stamboulis, R.V. Law, Characterization of fluorine containing glasses by ^{19}F, ^{27}Al, ^{29}Si and ^{31}P MAS-NMR spectroscopy, J. Dent. 34 (2006) 525–532.
[34] C. Rong, K.C. Wong-Moon, H. Li, P. Hrma, H. Cho, Solid state NMR investigation of phosphorus in aluminoborosilicate glasses, J. Non-Cryst. Solids 223 (1998) 32–42.
[35] F. Muñoz, L. Montagne, L. Delevoye, A. Durán, L. Pascaul, S. Cristol, J.F. Paul, Phosphate speciation in sodium borosilicate glasses studied by nuclear magnetic resonance, J. Non-Cryst. Solids 352 (2006) 2958–2968.
[36] H. Grussaute, L. Montagne, G. Palavit, J.L. Bernard, Phosphate speciation in Na_2O–CaO–P_2O_5–SiO_2 and Na_2O–TiO_2–P_2O_5–SiO_2 glasses, J. Non-Cryst. Solids 263, 264 (2000) 312–317.
[37] J.F. Stebbins, S. Kroecker, S.K. Lee, T.J. Kiczenski, Quantification of five- and six-coordinated aluminum ions in aluminosilicate and fluoride-containing glasses by high-field, high-resolution ^{27}Al NMR, J. Non-Cryst. Solids 275 (1–6) (2000) 2425–2432.
[38] D.R. Neuville, L. Cormier, D. Massiot, Al environment in peraluminous glasses: a ^{27}Al MQ-MAS, Raman and XANES investigation, Geochim. Cosmochim. Acta 68 (24) (2004) 5071–5079.
[39] Lin-Shu Du, J.F. Stebbins, Solid state NMR study of metastable immiscibility in alkali borosilicate glasses, J. Non-Cryst. Solids 315 (2003) 239–255.
[40] N.J. Clayden, S. Eposito, U.A. Jayasooriya, J. Sprunt, P. Pernice, Solid state ^{29}Si NMR and FT Raman spectroscopy of the devitrification of lithium metasilicate glass, J. Non-Cryst. Solids 224 (1998) 50–56.
[41] J.E. Shelby, Introduction to Glass Science and Technology, Royal Society of Chemistry, 1997, pp. 86–89.
[42] M.G. Mortuza, M.R. Ahsan, R. Dupree, D. Holland, Disproportionation of Q_m ($0 \le m \le 4$) species in partially devitrified $Li_2Si_2O_5$ glasses with small amounts of P_2O_5, J. Mater. Sci. 42 (2007) 7950–7955.
[43] S. Sen, Z. Xu, J.F. Stebbins, Temperature dependent structural changes in borate, borosilicate and boroaluminosilcate liquids: ^{11}B, ^{29}Si and ^{27}Al NMR studies, J. Non-Cryst. Solids 226 (1998) 29–40.